European Journal of Pharmaceutics and Biopharmaceutics 77 (2011) 297–305

Contents lists available at ScienceDirect

European Journal of Pharmaceutics and Biopharmaceutics

journal homepage: www.elsevier.com/locate/ejpb

Research paper

Ethylene vinyl acetate as matrix for oral sustained release dosage forms produced via hot-melt extrusion

A. Almeida [a], S. Possemiers [b], M.N. Boone [c], T. De Beer [d], T. Quinten [a], L. Van Hoorebeke [c], J.P. Remon [a], C. Vervaet [a,*]

[a] Laboratory of Pharmaceutical Technology, Ghent University, Ghent, Belgium
[b] Laboratory of Microbial Ecology and Technology, Ghent University, Ghent, Belgium
[c] Centre for X-ray Tomography (UGCT), Department of Physics and Astronomy, Ghent University, Ghent, Belgium
[d] Laboratory of Pharmaceutical Process Analytical Technology, Ghent University, Ghent, Belgium

ARTICLE INFO

Article history:
Received 23 June 2010
Accepted in revised form 6 December 2010
Available online 17 December 2010

Keywords:
Hot-melt extrusion
Ethylene vinyl acetate
Sustained release
Multiple-unit dosage form
Matrix system
Metoprolol tartrate

ABSTRACT

Different ethylene vinyl acetate grades (EVA9, EVA15, EVA28 and EVA40 having a VA content of 9%, 15%, 28% and 40%, respectively) were characterized via differential scanning calorimetry. Glass transition temperature (T_g), polymer crystallinity, melting point and polymer flexibility were positively influenced by the vinyl acetate content. The processability of EVA-based formulations produced by means of hot-melt extrusion (2 mm die) was evaluated in function of VA content, extrusion temperature (60–140 °C) and metoprolol tartrate (MPT, used as model drug) concentration (10–60%). Matrices containing 50% MPT resulted in smooth-surfaced extrudates, whereas at 60% drug content severe surface defects (shark skinning) were observed. Drug release from EVA/MPT matrices (50/50, w/w) was affected by the EVA grades: 90% after 24 h for EVA15 and 28, while EVA9 and EVA40 formulations released 80% and 60%, respectively. Drug release also depended on drug loading and extrusion temperature. For all systems, the total matrix porosity (measured by X-ray tomography) was decreased after dissolution due to elastic rearrangement of the polymer. However, the largest porosity reduction was observed for EVA40 matrices as partial melting of the structure (melt onset temperature: 34.7 °C) also contributed (thereby reducing the drug release pathway and yielding the lowest release rate from EVA40 formulations).

The Simulator of the Human Intestinal Microbial Ecosystem (SHIME) used to evaluate the stability of EVA during gastrointestinal transit showed that EVA was not modified during GI transit, nor did it affect the GI ecosystem following oral administration.

1. Introduction

Hot-melt extrusion (HME) is a well-known technique in the field of polymer science, and it has proven to be a useful tool for pharmaceutical purposes to develop immediate- or sustained-release formulations. Compared with other techniques, HME has a lower environmental impact (absence of solvents) and reduced costs (few processing steps, continuous operation) [1–3]. As sustained release dosage forms have an important role to improve the life quality of chronic and poly-medicated patients by reducing their daily intake of dosage forms, considerable research efforts have been directed towards the use of polymers that provide practical, safe and controlled long-term delivery of drugs. Several polymers, suitable for pharmaceutical HME applications have been identified (ethylcellulose, polymethacrylate, hydroxypropylcellulose, polyethylene oxide, polyvinylalcohol, etc.) [4–7], but the majority of them require a plasticizer to improve the elasticity and flexibility of the polymers [8–11]. This results in several restrictions related to polymer/plasticizer miscibility, plasticizer concentration, interactions with drug and polymer. In contrast, ethylene vinyl acetate (EVA) does not require a plasticizer to obtain good quality extrudates.

EVA is a copolymer of ethylene and vinyl acetate (VA). While polyethylene is a semicrystalline polymer with alternating crystalline lamellae (with different types of crystals) and amorphous domains, the incorporation of VA co-monomer units (typically the VA content varies between 9% and 40%) into a polyethylene backbone chain induces differences in crystallinity and crystalline structure, melting point, solubility, density and glass transition temperature, affecting the flexibility and thermoplastic characteristics of EVA [12,13]. Therefore, the versatility of EVA for hot melt processing resulted in a wide spectrum of applications [14]. In the pharmaceutical field, it has been specifically used for the development of films

* Corresponding author. Address: Laboratory of Pharmaceutical Technology, Ghent University, Ghent, Belgium. Tel.: +32 (0) 9 264 8069.
E-mail address: Chris.Vervaet@UGent.be (C. Vervaet).

0939-6411/$ - see front matter © 2010 Elsevier B.V. All rights reserved.
doi:10.1016/j.ejpb.2010.12.004

[15,16], stent coatings [17], implantable devices [18], vaginal rings [19], etc.

The purpose of this study was to evaluate the potential of EVA as a matrix carrier for oral sustained release dosage forms produced via hot-melt extrusion, and to characterize the different aspects of EVA copolymers. Metoprolol tartrate was embedded as model drug in the EVA matrices.

As the stability of EVA matrices after oral intake when exposed to the gastrointestinal fluids and its effects on the gastrointestinal microbiota have not been described, the effect of the polymer on the gastrointestinal ecosystem and vice versa was evaluated using a Simulator of the Human Intestinal Microbial Ecosystem (SHIME).

2. Material and methods

2.1. Materials

Different ethylene vinyl acetate (EVA) grades (Elvax® 40w, 260, 550 and 750 with a vinyl acetate (VA) content of 40, 28, 15 and 9 wt.%, respectively) were kindly donated by Dupont (Geneva, Switzerland) and used as hydrophobic carrier. Metoprolol tartrate (MPT) (10 μm) (EQ Esteve, Barcelona, Spain) was selected as model drug.

2.2. Hot-melt extrusion: production of the mini-matrices

EVA powder and physical mixtures of metoprolol tartrate and EVA (homogenized using mortar and pestle) were fed into a co-rotating twin-screw mini-extruder (Haake MiniLab II Micro Compounder, Thermo Electron, Karlsruhe, Germany), operating at different screw speeds (40, 60 and 90 rpm) and processing temperatures (60, 80, 90, 100, 110, 120, 130 and 140 °C) in order to evaluate the processability of these formulations via hot-melt extrusion. The extruder was equipped with a pneumatic feeder, two archimedes screws and a cylindrical die of 2 mm. The extrudates were cooled down to room temperature and manually cut, using surgical blades, into mini-matrices of 2 mm length.

2.3. Extrudate characterization

The extrudates were visually inspected for surface defects (e.g. shark skinning). The deformation due to cutting and the presence of cracks were evaluated using a KH-7700 digital microscope (Hirox, Japan), equipped with a high resolution zoom lens (MXG-10C model, using co-axial vertical lighting for high-level optical observation) and an OL-70 II objective lens with a magnification capacity of 70–700×. The imaging system had a 2.11 mega-pixel CCD sensor and a maximum pixel resolution of 30 mega-pixels (i.e. 6400 horizontal lines and 4800 vertical lines). To visualize the surface morphology photomicrographs were taken with a field emission gun scanning electron microscope (SEM, type Quanta 200F, FEI, Eindhoven, Nederland). The pressure in the chamber was 100 Pa, and a large field detector was used.

2.4. X-ray diffraction

The crystallinity of powdered EVA grades and EVA samples extracted from the intestinal passage experiment was investigated by means of X-ray diffraction. The X-ray patterns were determined using a D5000 Cu Kα diffractor (λ = 0.154 nm) (Siemens, Karlsruhe, Germany) with a voltage of 40 mA in the angular range of $10° < 2\theta < 60°$ using a step scan mode (step width = 0.02°, counting time = 1 s/step).

2.5. Raman spectroscopy

The MPT crystallinity and distribution of and the EVA40 solid state were evaluated in EVA matrices containing 50% MPT via Raman microscopy. A RamanRxn 1 Microprobe (Kaiser Optical systems, Ann Arbor, USA) equipped with an air-cooled CCD detector (back-illuminated deep depletion design) was used to inspect MPT crystallinity in the tablets. Using a 10× long working distance objective lens (spot size of 50 μm), 10 spectra were collected on a vertical cross-section of the tablets. To evaluate the MPT distribution on the vertical cross-section, three areas ($2200 \times 1200\ \mu m^2$) (two at the edges and one in the middle of the mini-tablet) were scanned in a point-by-point mapping mode with a step size of 50 μm in both x and y directions. The laser wavelength during the experiments was the 785 nm line from a 785 nm Invictus NIR diode laser. All spectra were recorded at a resolution of 4 cm^{-1} using a laser power of 400 mW and a laser light exposure time of 20 s per spectrum. Before data analysis, spectra were baseline-corrected (Pearson's method). Data collection and analysis were done using the HoloGRAMS™ data collection software package, the HoloMAP™ data analysis software package and the Matlab® software package (version 6.5).

2.6. Thermal analysis

Thermogravimetric analysis (Hi-res TGA 2950, TA instruments, Leatherhead, UK) was employed to investigate the thermal stability of EVA, MPT and extruded EVA/MPT samples (50/50 ratio, w/w). Samples (±15 mg) were equilibrated at 50 °C and heated to 500 °C at a heating rate of 10 °C/min while recording the weight loss.

Glass transition temperature (T_g), crystallization temperature (T_c), melting point (T_m) and heat of fusion (ΔH) of pure components (EVA40, EVA28, EVA15, EVA9 and MPT), physical mixtures and extruded samples were analyzed by differential scanning calorimetry (DSC) and modulated differential scanning calorimetry (MDSC). The DSC instrument used was a Model 2920 from TA Instruments (Leatherhead, UK) running in standard mode and equipped with a refrigerated cooling system (RCS). Samples (±10 mg) were run in closed aluminium pans; the mass of each empty sample pan was matched with the mass of the empty reference pan to ±0.10 mg. Depending on the samples and the determined parameters, the experimental method consisted of a single heating cycle (heating rate of 20 °C/min from −100 to 180 °C) or a three-phase analysis with consecutive heating, cooling and heating cycles. All samples and starting materials were analyzed in triplicate.

MDSC measurements were carried out using a Q2000 Modulated DSC (TA, Instruments, Leatherhead, UK) equipped with a refrigerated cooling system. Dry nitrogen at a flow rate of 50 ml/min was used to purge the DSC cell. The amplitude of the temperature was 0.3 °C, the period was 50 s and the underlying heating rate was 2 °C/min. The samples were evaluated according to the three cycle analysis (heating, cooling and heating) from −100 to 180 °C.

All results were analyzed using the TA Instruments Universal Analysis 2000 software.

2.7. In vitro drug release

Drug release from the EVA-based matrices was determined using USP apparatus 1 (baskets), in a VK 7010 dissolution system combined with a VK 8000 automatic sampling station (VanKel Industries, New Jersey, USA). The mini-tablets (eight tablets of 2 mm length) were placed in demineralized water (900 ml, at a temperature of 37 ± 0.5 °C), while the rotational speed of the baskets was 100 rpm. Samples of 5 ml were withdrawn at 0.5, 1, 2,

4, 6, 8, 12, 16, 20 and 24 h (without medium replacement) and spectrophotometrically analyzed for MPT at 222 nm by means of a Perkin–Elmer Lambda 12 UV–VIS double beam spectrophotometer (Zaventem, Belgium). The metoprolol tartrate content in the samples was determined by linear regression using a calibration curve. Each batch was evaluated in triplicate.

2.8. X-ray tomography

The internal 3D-structure of the mini-matrices (total porosity, maximum opening and equivalent diameter of the pores) was evaluated by means of X-ray tomography. Total porosity is expressed as the percentage of a material's pore volume to its total volume. Equivalent diameter and maximum opening are the diameter of a sphere with the same volume as the pore and the diameter of largest sphere that can be inscribed in the pore, respectively.

Extruded EVA 40 samples and mini-matrices containing EVA9, 15, 28 and 40 in combination with 50% MPT were scanned before and after 24 h dissolution testing with the high resolution micro-CT scanner of the Ghent University Centre for X-ray Tomography. The EVA40 sample was also evaluated after 72 h dissolution testing. The system is composed of a Feinfocus X-ray tube with Tungsten transmission target and diamond exit window, a Micos high precision airbearing rotation stage and a Varian Paxscan 2520 V a-Si flat panel detector [20]. The sample was rotated over 360° in 0.36° steps, with radiographic images recorded at every step. The 1000 shadow images were processed and reconstructed to 1500 cross-sectional images of 1100 × 1100 pixels with Octopus software. Additional reconstructions using the Modified Bronnikov Algorithm (MBA) [21–22] and the Bronnikov Aided Correction (BAC) [23] were performed, to reduce the phase artefacts. As the voxel pitch was about 2 μm, pores with a smaller diameter were not visible on the CT scans. However, they do affect the reconstructed image by reducing the density inside that voxel.

2.9. Stability of the EVA40 polymer under gastrointestinal conditions

The stability of EVA40 upon oral ingestion was evaluated in the Simulator of the Human Intestinal Microbial Ecosystem (SHIME), developed by the Laboratory of Microbial Ecology and Technology, Ghent University, as described earlier [24]. In brief, EVA40 polymer (2 g/l) was added to a standardized nutritional medium and incubated under simulated stomach conditions for 90 min (37 °C, aerophilic conditions). Next, an appropriate amount of bile salts and digestive enzymes was added to simulate small intestinal conditions, and the samples were further incubated for 150 min (37 °C, microaerophilic conditions). Finally, a complex microbial community was taken from the ascending colon compartment of the SHIME and added to the setups. The samples were further incubated for a period of 48 h (37 °C, anaerobic conditions).

All experiments were performed in triplicate. As a control, the same experiment was performed in parallel, without addition of EVA40.

EVA40 polymer was isolated from the stomach and small intestinal incubation medium, and the polymer's integrity and structure was analyzed by means of DSC, X-ray and SEM. EVA40 could not be recovered from the colonic incubation samples as the medium was too dirty for EVA40 isolation.

The potential breakdown of the polymer by the intestinal microflora was indirectly assessed. Changes in composition or activity of the microbial community in the test with EVA40 as compared to the control were used as marker for interaction between EVA40 and the intestinal microbiota. Changes in composition were assessed by selective plate counting for different bacterial groups and by PCR–DGGE (Denaturing Gradient Gel Electrophoresis) analysis of the total microbial community, as described by Possemiers et al. [25]. Effects on microbial activity were evaluated by pH measurements and by quantification of the concentrations of short-chain fatty acids (SCFA) and ammonium in the samples at the beginning and end of the colonic incubations, as described earlier [25].

3. Results and discussion

3.1. Polymer thermal analysis (influence of VA content)

Thermal investigation of the EVA grade (EVA40, EVA28, EVA15 and EVA9), with different vinyl acetate content (40%, 28%, 15% and 9%, respectively), resulted in distinct thermograms (Fig. 1A and Table 1).

The glass transition temperature (T_g) was not significantly affected by the VA content, ranging between −25.3 °C for EVA15 and −28.7 °C for EVA40. Such a low T_g is responsible for the polymer rubbery state at room temperature (high flexibility). However, the specific heat capacity change (ΔCp) during glass transition increased with the VA content (Fig. 1B). This is explained by the complex amorphous phase of EVA that consists of an interfacial (less mobile) and a melt-like (very mobile) amorphous phase [13]. The free movement of amorphous segments during glass transition contributes to the change of the specific heat. When a part of the amorphous segments is locked (less mobile) between the crystalline chains or does not contribute to the glass transition change, the change of heat capacity is reduced [26]. Hence, the results indicate that EVA with a higher VA content has a lower rigid amorphous content, responsible for a higher flexibility (confirmed by handling the polymer).

Distinct VA grades were also responsible for differences in the melting onset temperatures and melting peaks. EVA40 showed three melting peaks (three crystalline forms confirmed by the derivative (time) of the heat flow), a melt onset temperature at 34.9 °C and a low heat of fusion (ΔH calculated from the integration of the three peaks) (Table 1). MDSC analysis of EVA40 indicated that a small part of the crystalline phase already melted at room temperature (partial melting of the polymer), whereas the majority of the crystals melted at 42.8 °C (T_m).

According to Wang et al. [13], three different types of crystals can be detected in EVA polymer with 18% VA content. However in our study, only two polymorphs were visualized for EVA28, 15 and 9, which in the case of EVA28 were present in similar proportions (Fig. 1A). Furthermore, ΔH measurements indicated that a lower VA content increased the crystallinity of the polymer. These results were also supported by X-ray diffraction (Fig. 2).

According to these thermoanalyses, the incorporation of vinyl acetate co-monomer units into a polyethylene backbone chain has three main critical effects: (a) reduced crystallinity, (b) lower melting point and (c) increased flexibility.

3.2. Processability of EVA polymers via hot-melt extrusion

Depending on their VA content, the extrusion behavior of the EVA grades differed: while EVA40 and EVA28 could already be processed at a temperature of 60 °C (with higher torque registered for EVA28), a temperature of 100 and 110 °C was required for EVA15 and EVA9, respectively. These results were correlated with the melting (onset) melting temperature observed for the different EVA grades (Table 1). For example, at 60 °C EVA28 was only partially melted, justifying the higher torque.

Molecular weight measurements showed that EVA samples that contained a lower VA content presented a higher molecular weight (Table 1), responsible for an increase in polymer melt viscosity. Therefore, higher process temperatures aided the extrusion

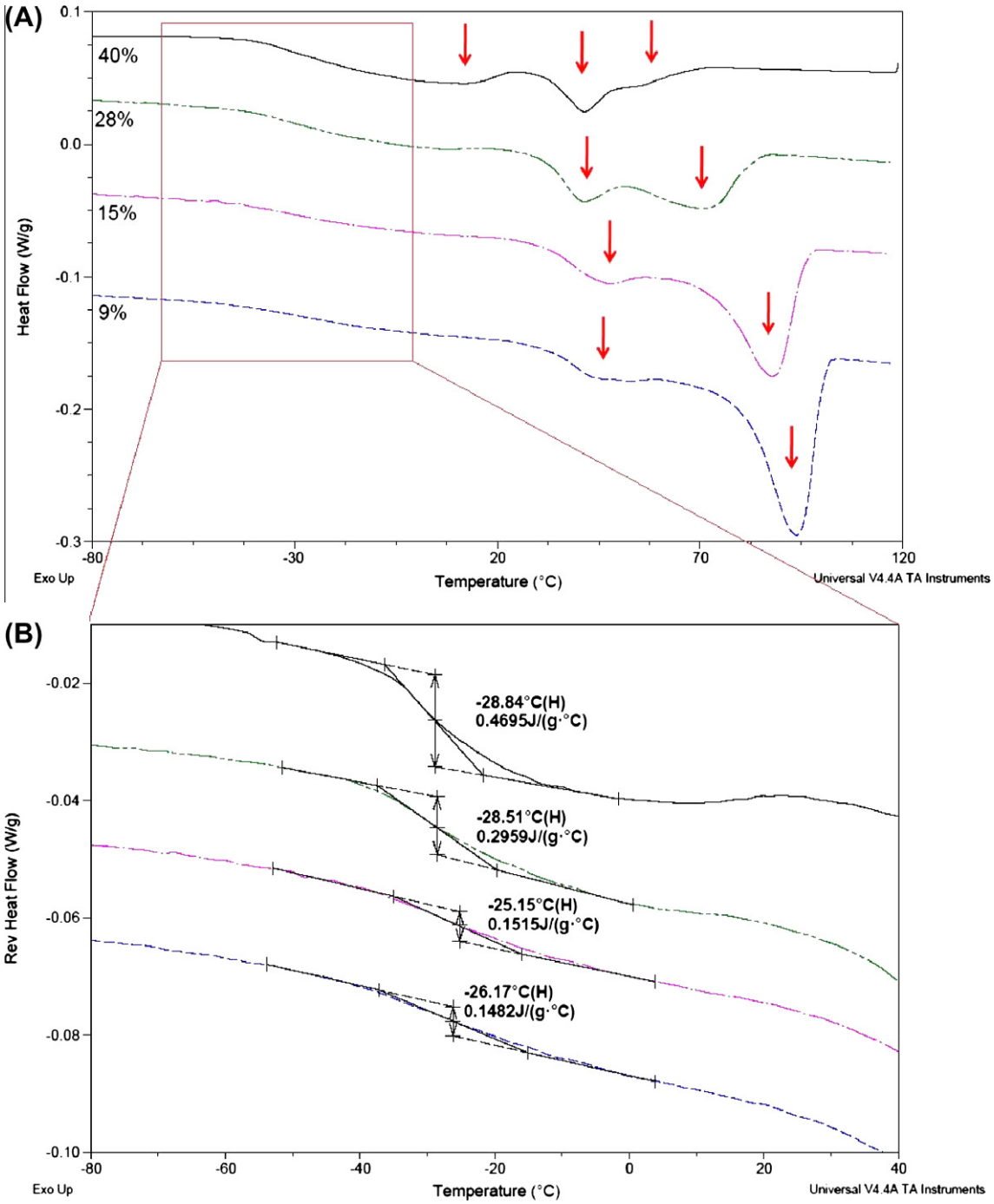

Fig. 1. (A) Thermograms of EVA with four different VA content (9%, 15%, 28% and 40%). The DSC was executed with a heat flow of 10 °C/min. The arrows indicate three crystal forms for EVA40 and 2 for EVA9, 15 and 28. (B) Detail of EVA polymers T_g exhibiting different ΔCp. (For interpretation of the references to color in this figure legend, the reader is referred to the web version of this article.)

Table 1
General properties, thermal behavior and crystallinity of the four different types of EVA.

General properties				DSC: thermal behavior and crystallinity		
Polymer type	%VA	MW	T_g (°C)	Melt onset temp. (°C)	T_m (°C)	Crystallinity (%)[a]
EVA40	40	64,900	−28.7 ± 0.3	34.9 ± 0.3	42.8 ± 0.0	13.7
EVA28	28	101,600	−28.6 ± 0.5	38.6 ± 1.1	72.8 ± 0.9	17.1
EVA15	15	151,200	−25.3 ± 0.5	70.0 ± 0.1	91.1 ± 0.1	29.4
EVA9	9	578,200	−26.9 ± 1.2	80.2 ± 0.1	98.6 ± 0.2	33.1

[a] Crystallinity was calculated with reference to the enthalpy of fusion (ΔH_f^*) of the perfect polyethylene (PE) crystal (277.1 J/g), with the following formula: $Xc = (\Delta H_f / \Delta H_f^*) \times 100$. ΔH_f = enthalpy of fusion of the respective EVA.

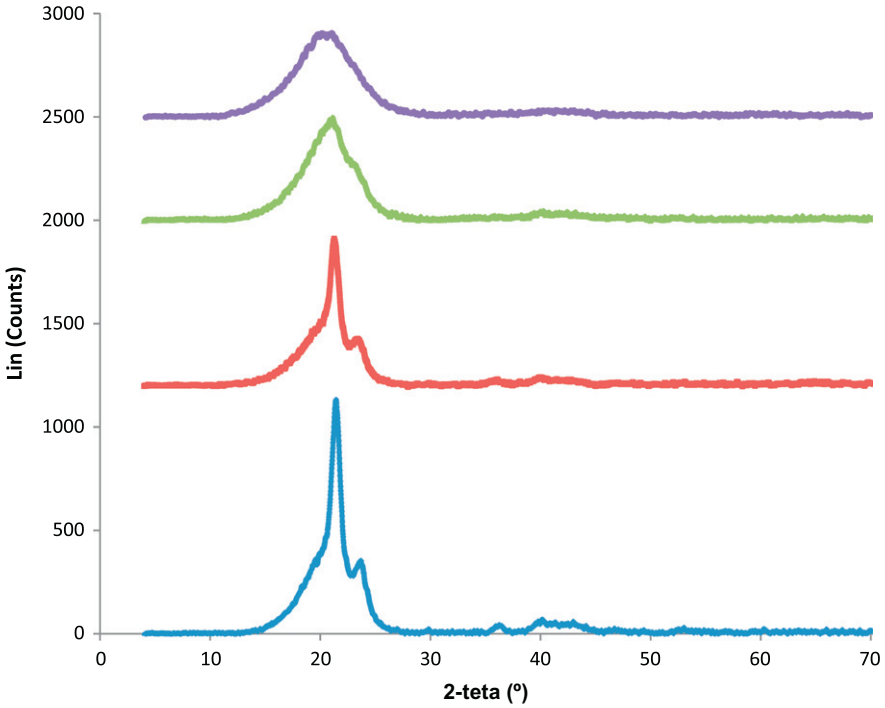

Fig. 2. X-ray diffraction of the four different types of EVA. From the top to the bottom: EVA40, EVA28, EVA15 and EVA9.

process by lowering the flow viscosity of the polymers with lower VA contents.

TGA experiments proved that EVA was stable at all processing temperatures as degradation only occurred above 250 °C. All extrudates had a smooth surface and were transparent, except EVA9 that was slightly opaque after extrusion.

The addition of metoprolol tartrate (MPT) to the EVA formulation affected the morphology of the extrudates: up to 50% MPT load, EVA40 extrudates had a smooth surface, while at 60% drug content the matrices showed severe shark skinning. EVA40 formulations containing 50% MPT were easily processed between 60 and 120 °C (although the higher melt viscosity of the formulation below 70 °C resulted in a high torque during extrusion), whereas EVA15 and EVA9 required an extrusion temperature above 100 °C to avoid shark skinning. However, a temperature higher than 123 °C (i.e. melting point of MPT) was excluded from the experiments in order to avoid the formation of a glass solution (thermodynamically instable) and a lower morphologic quality of the extrudates.

After extrusion at 90 °C, DSC thermograms of the extrudates showed that extrusion did not change the polymer structure and that the drug was mostly in the crystalline form based on ΔH of pure MPT and physical powder mixtures (Fig. 3). Despite the higher melting point of MPT (123 °C), a limited amount of MPT (±15%) melted during extrusion at 90 °C (possibly due to the friction heat generated during processing) and did not recrystallize upon

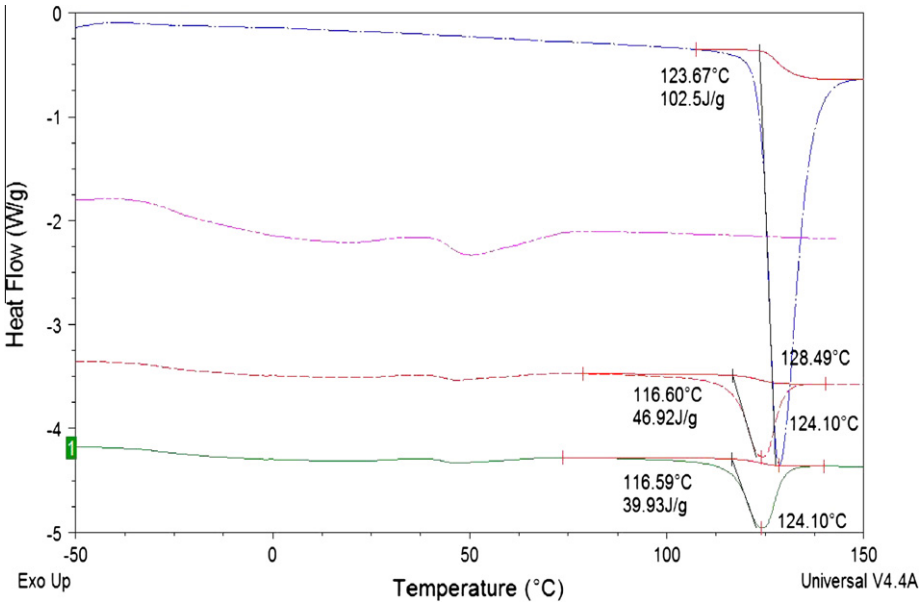

Fig. 3. DSC thermograms of pure MPT (1), EVA40 (2), physical mixture (3) and extrudate of EVA40 and MPT (EVA/MPT, w/w, 50/50) (4).

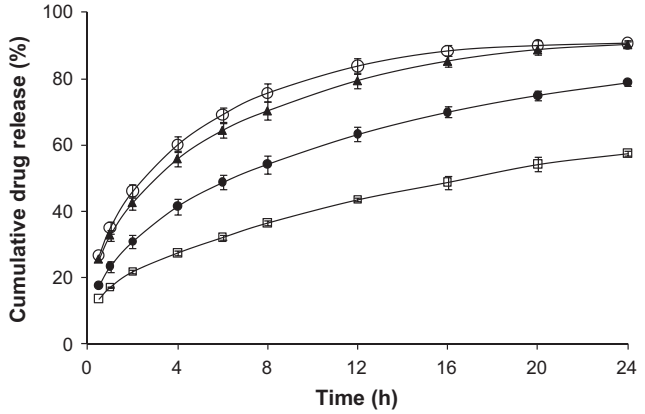

Fig. 4. Cumulative drug release of MPT from EVA40 (□), EVA28 (▲), EVA15 (○) and EVA9 (●) matrices (EVA/MPT, w/w, 50/50).

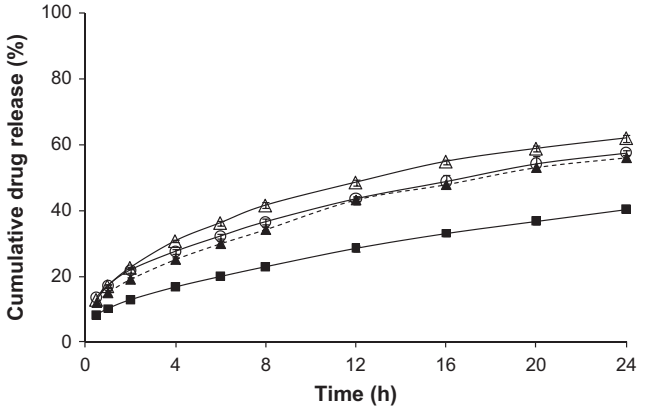

Fig. 6. Cumulative drug release of MPT from EVA40/MPT matrices (50/50, w/w) processed at 60 °C (■), 80 °C (▲), 90 °C (○) and 100 °C (Δ).

cooling. The thermogram of a mixture of amorphous MPT and EVA polymer (1:1) showed two distinct glass transitions at the same temperatures as the pure forms, indicating that drug and polymer were not miscible.

Raman spectroscopy indicated that crystalline drug was homogeneously dispersed in the polymer matrix.

Drug release from EVA/MPT matrices (50/50, w/w) was affected by the EVA grades (Fig. 4) as the release increased in the following order: EVA15, EVA28, EVA 9 and EVA40. EVA15 and 28 registered a faster MPT release after 24 h of dissolution (90%), whereas for EVA9 and EVA40 the release was limited to 80% and 60%, respectively. The release profiles of all extruded mini-matrices indicated a small burst effect during the first hour, followed by a slower release.

Drug release rate also depended on drug loading (7% and 58% release after 24 h for EVA40 formulations containing 10% and 50% MPT, respectively; Fig. 5) and extrusion temperature (Fig. 6). No significant differences were detected in a temperature range between 80 and 100 °C (around 60% of MPT released after 24 h), whereas at lower extrusion temperatures the release was considerably lower (40%). The enthalpy of fusion (measured via DSC) indicated that the entire drug fraction remained crystalline at an extrusion temperature of 60 °C, whereas the crystallinity of drug fraction was reduced at higher process temperatures: 85%, 87% and 74% remaining crystallinity at 80, 90 and 100 °C, respectively. Using an extrusion temperature of 110 °C resulted in an EVA matrix containing only 50% of crystalline drug phase; however, the release properties of these matrices were not tested due to the poor quality of the extrudates. The extrusion rate (varied by means of the screw speed) did not affect drug release (data not shown).

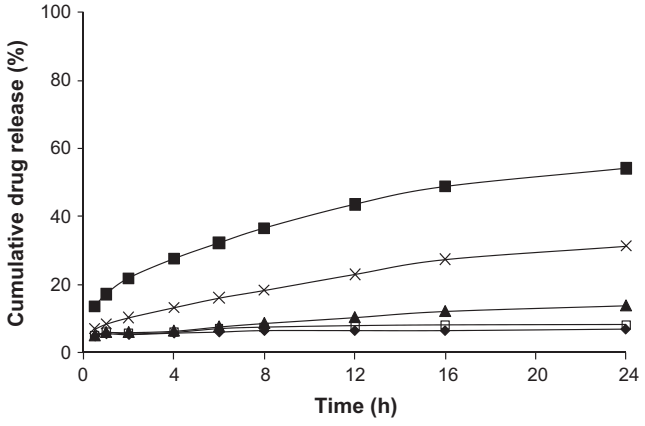

Fig. 5. Cumulative drug release of MPT from EVA40/MPT matrices containing different drug loadings: 10% (♦), 20% (□), 30% (▲), 40% (×) and 50% (■).

None of the matrices achieved complete release after 24 h, indicating that a fraction of the drug was trapped inside the matrix, with a higher impact at low drug loadings. At high drug loadings, the drug was able to diffuse through the matrix, as the porous network is connected with the surface, allowing the drug to be released. As no porosity was detected by SEM on extruded matrices consisting of pure EVA (Fig. 9B), the porous network path seems to be created by drug crystals. Once exposed to the dissolution medium, the water penetrates into the hydrophobic polymer matrix and the dispersed crystalline drug is dissolved and released by means of percolation, leaving behind an empty porous EVA carcass (a system described by several authors regarding EVA films studies) [27–29].

These results and the aforementioned observations clearly indicated that the drug release mechanism from EVA matrices is a complex combination of different parameters, such as drug crystallinity, polymer crystallinity (related with the VA content), drug loading (responsible for the porosity in the matrix) and extrusion temperature (affecting the proportion between amorphous and crystalline systems).

As (M)DSC experiments indicated that a higher VA content lowered the crystallinity of EVA polymer (Table 1), the highest release rate was expected from EVA40. According to literature [30] a reduction in polymer crystallinity increases its permeability and diffusivity. However, the slower MPT release from EVA40 compared to the other EVA formulations indicates that other parameters besides crystallinity were affecting drug release from EVA matrices. To elucidate these phenomena, the matrix geometry (porosity and pore topology) of extruded EVA matrices was further characterized via X-ray tomography and SEM.

3.3. Matrix porosity

Matrix porosity was evaluated on samples before and after 24 h dissolution experiments, and EVA40 matrices were also evaluated after 72 h dissolution. These results were cross-linked with the drug release profiles in order to establish a possible correlation between both observations.

X-ray tomography measurements showed a cylindrical matrix characterized by a white/grey area (denser material corresponding to small crystals of drug, EVA polymer and lower presence of sub-resolution porosity) in which black spots can be distinguished (Fig. 7)) representing the pores in the EVA matrices after hot-melt extrusion. Porosity measurements indicated similar values for all matrices formulated with different EVA grades, ranging from

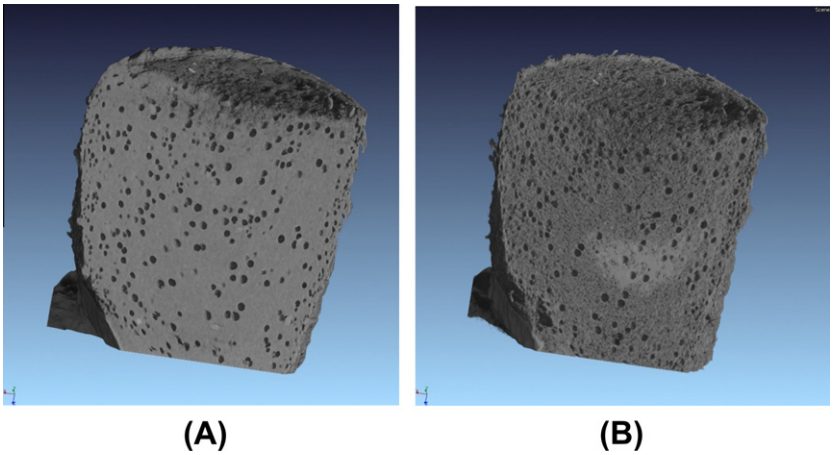

Fig. 7. X-ray tomography scan of an EVA28 matrix (A) before and (B) after 24 h dissolution. (For interpretation of the references to color in this figure legend, the reader is referred to the web version of this article.)

Table 2
Total porosity and mean equivalent diameter (determined by X-ray tomography) of the EVA matrices, before and after 24 h of dissolution experiments.

	EVA40	EVA28	EVA15	EVA9
Total porosity (%)				
Before dissolution	7.2	5.2	8.9	7.6
After dissolution	6.9	8.3	12.9	9.5
Δ porosity	−0.3	3.1	4.0	1.9
Mean equivalent diameter				
Before dissolution	25.3 ± 12.5	30.2 ± 14.9	51.0 ± 24.1	55.2 ± 32.6
After dissolution	26.1 ± 14.6	29.6 ± 17.0	30.1 ± 22.7	33.7 ± 28.4

5.2% (EVA28) to 8.9% (EVA15), whereas the mean equivalent diameter registered higher values for EVA matrices with lower VA content (55.2 and 51.0 μm for EVA9 and EVA15, respectively) (Table 2). X-ray tomography renderings confirmed that larger pores were located in the center of the matrices (orange and red colors in Fig. 8B and C), while a higher concentration of small pores was registered just below the surface of the matrices, probably due to compression of the material during passage through the die.

Although 50% of the EVA matrices were composed of drug and at least 60% of the drug was released from these matrices after

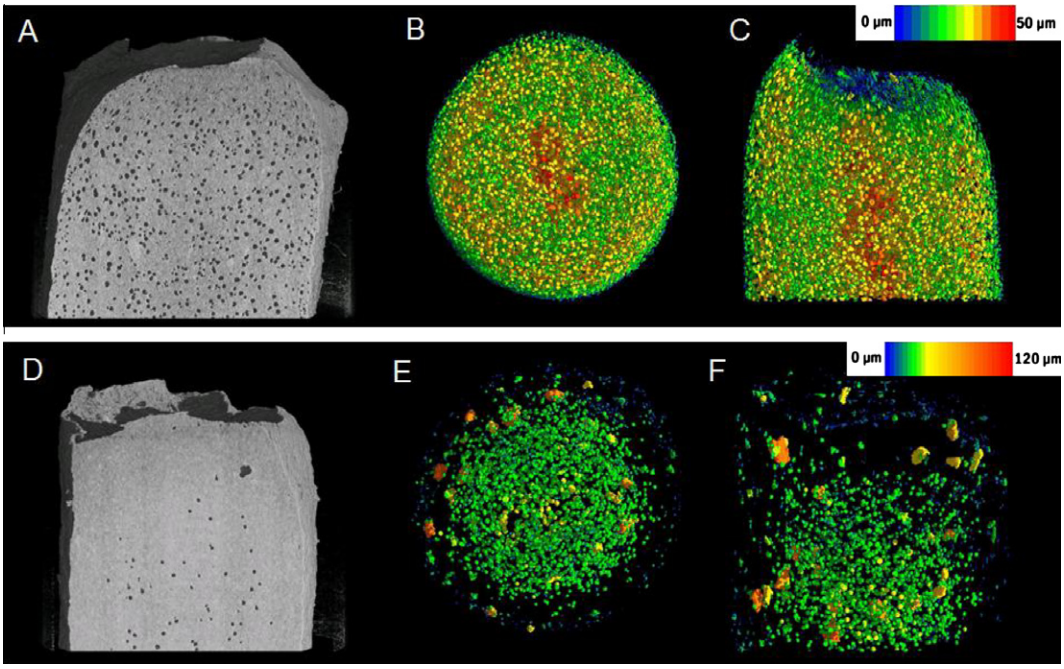

Fig. 8. X-ray tomography renderings of EVA40 matrices with 50% of MPT. Axial (A and C) and radial (B) cross-sections before dissolution, axial cross-section after 24 h dissolution, axial (F) and radial (E) cross-sections after 72 h dissolution. Black spots (A and D) indicate pores. The color scale used in (B, C, E and F) represents the pore size (maximum opening), blue representing small pores, red representing larger pores. (For interpretation of the references to color in this figure legend, the reader is referred to the web version of this article.)

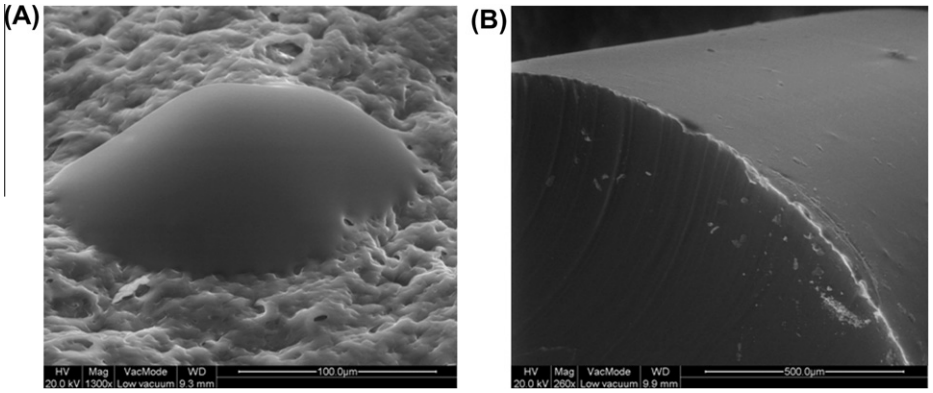

Fig. 9. (A) Surface structure of EVA40 matrix containing 50% MPT after 72 h dissolution (scale bar: 100 μm). (B) Surface structure of pure EVA after hot-melt extrusion at 90 °C (scale bar: 500 μm).

24 h (Fig. 4), a limited increase in porosity was observed for EVA 9, 18 and 28 after 24 h dissolution testing. In case of EVA40 matrices, even a small reduction in matrix porosity was observed after dissolution testing (Table 2).

X-ray tomography renderings of EVA40 matrices indicated that the matrix was characterized by a significant structural change after dissolution: after 24 h dissolution the pore structure had partially collapsed (Fig. 8D after 24 h dissolution vs. Fig. 8A before dissolution). Additionally, axial and radial cross-sections after 72 h dissolution testing (using a color scale to represent different pore sizes) indicated a considerable reduction in porosity, especially in the area closer to the surface (Fig. 8E and F). SEM images of these matrices (Fig. 9) confirmed these results, suggesting that the EVA40 matrix was initially (i.e. after hot-melt extrusion) structurally supported by drug crystals. As the flexible polymer framework does not have sufficient rigidity to maintain its form once part of the drug has leached from the tablet, the structure collapses, resulting in a reduction in the number of pathways available for drug release. This event was also observed for EVA28 matrices, but to a lesser extent (Fig. 7). The insufficient rigidity of the matrix resulted in elastic rearrangement of the polymer chains, reducing the pores size and contributing for the sustained release of the drug.

The lower dissolution rate from EVA40 matrices compared to the other EVA grades (Fig. 4), despite its lower crystallinity (Table 2), is due to molecular rearrangement of this EVA grade (in addition to elastic recovery of the polymer chains). After 72 h dissolution testing, small blobs that resembled the structure of hot-melt extruded, non-porous, pure EVA (Fig. 9) were identified on the surface of the EVA matrices, effectively reducing the total matrix porosity to 1.0%. As MDSC experiments confirmed that partial melting of this polymer occurred below 37 °C (Table 1), molecular rearrangements was possible, thus eliminating part of the pores. Therefore, EVA40 experiences two distinct events during drug release: elastic recovery of the polymer and a molecular rearrangement (partial melting) of the crystalline phase. As a result, the sustained drug release capacity is increased (Fig. 4).

The collapse of the EVA40 matrices was also macroscopically observed as the volume of these matrices significantly ($p < 0.001$) decreased by 24%, in contrast the volume change of EVA28 matrices was limited to 6.2% (not statistically significant).

3.4. Stability of EVA in the gastrointestinal tract

The toxicology of EVA-based systems has been widely investigated for its use in implants and vaginal rings for controlled release of female contraceptives [18]. These studies confirmed its safety and efficacy for these applications. However, upon oral intake of EVA polymers, the product passes the intestinal environment, in which chemical or enzymatic modifications may occur, affecting its safety. Moreover, the human colon is colonized by a complex microbial community, which may modify the EVA structure and may in turn be influenced by the exposure to the product. As such effects have not yet been explored, EVA40 (2 g; i.e. 10-fold higher compared to the anticipated maximum daily oral intake of 200 mg) was incubated with different GI fluids in the SHIME system, to determine its intestinal stability and potential impact on microbial metabolism indicators (pH, ammonium and fatty acids) (Table 3) and DNA profile of several types of bacteria. EVA40 was selected as test specimen based on its high VA content, as the co-monomer shows more potential for interaction [18]. No significant differences in bacterial count were observed, except some minor changes in total aerobes ($p < 0.05$). The metabolism and DNA profile of the GI microbiota were not affected by exposure to EVA40 (DGGE profiles of the bacteria in the control and treatment samples had more than 80% similarity). The chemical structure of EVA40, after exposure to stomach and small intestine fluids, was not altered as DSC, X-ray diffraction, SEM and Raman spectroscopy showed similar thermal behavior, crystallinity, surface structure and chemical finger print, respectively. From the SHIME experiments, it can therefore be concluded that no evidence was found that EVA would be chemically or enzymatically modified after passage through the GI tract, nor were important changes in the activity or composition of the GI bacterial community observed after exposure to EVA.

Table 3
Results (pH, bacterial group, ammonium and fatty acid concentration) of the SHIME experiments after exposure of EVA40 to simulated intestinal fluid. The EVA concentration was 2 g/l in the treatment group; no EVA was used in the control group.

	Control	Treatment
Bacterial groups concentration [log (CFU ml^{-1})]		
Lactobacillus sp.	3.77 ± 0.22	3.53 ± 0.41
Clostridium sp.	7.11 ± 0.36	7.12 ± 0.12
Total aerobes*	7.74 ± 0.15	6.77 ± 0.24
Total anaerobes	7.95 ± 0.25	7.88 ± 0.07
Bifidobacterium	7.06 ± 0.27	6.84 ± 0.38
pH	6.45 ± 0.04	6.48 ± 0.08
Ammonium (mg NH_4^+-H/L)	158.31 ± 7.46	162.98 ± 4.94
Fatty acids (mmol/l)		
Acetate	1.32 ± 0.09	1.27 ± 0.09
Proprionate	6.55 ± 0.21	6.62 ± 0.20
Butyrate	4.62 ± 0.83	5.05 ± 0.12
Total SCFA	15.60 ± 1.08	16.11 ± 0.04
BSCFA	3.11 ± 0.14	3.16 ± 0.04

* Indicated a significant difference between control and treatment group ($p < 0.01$, $\alpha = 5\%$), with a mean difference of 9.46 CFU ml^{-1} for total aerobes.

4. Conclusion

EVA polymers proved to be promising matrix formers to manufacture oral sustained release tablets without the addition of a plasticizer. The VA content plays an important role in the solubility, crystallinity, elasticity and porosity of the extruded matrix, with significant impact on the drug release profile. Up to 50% MPT could be incorporated in the formulation, with a maximum of 90% drug released after 24 h.

These results also showed that EVA was not modified nor did it affect the GI ecosystem after exposure to the gastrointestinal fluids following oral administration.

Acknowledgements

The authors greatly acknowledge Els Verdonck (TA Instruments – Waters) and Prof. Dr. G.P. Andrews (Faculty of Pharmacy, Queen's University, Belfast) for their assistance with (M)DSC analysis and the polymer grinding, respectively. Sam Possemiers benefits from a post-doctoral scholarship of the Flemish Research Foundation (FWO-Vlaanderen).

References

[1] M.M. Crowley, F. Zhang, M.A. Repka, S. Thumma, S.B. Upadhye, S.K. Battu, J.W. McGinity, C. Martin, Pharmaceutical applications of hot-melt extrusion: part I, Drug Development and Industrial Pharmacy 33 (9) (2007) 909–926.
[2] M.A. Repka, S.K. Battu, S.B. Upadhye, S. Thumma, M.M. Crowley, F. Zhang, C. Martin, J.W. McGinity, Pharmaceutical applications of hot-melt extrusion: part II, Drug Development and Industrial Pharmacy 33 (10) (2007) 1043–1057.
[3] M.A. Repka, S. Majumdar, S.K. Battu, R. Srirangam, S.B. Upadhye, Applications of hot-melt extrusion for drug delivery, Expert Opinion on Drug Delivery 5 (12) (2008) 1357–1376.
[4] E. Verhoeven, T.R.M. De Beer, G. Van den Mooter, J.P. Remon, C. Vervaet, Influence of formulation and process parameters on the release characteristics of ethylcellulose sustained-release mini-matrices produced by hot-melt extrusion, European Journal of Pharmaceutics and Biopharmaceutics 69 (1) (2008) 312–319.
[5] M.A. Repka, T.G. Gerding, S.L. Repka, J.W. McGinity, Influence of plasticizers and drugs on the physical–mechanical properties of hydroxypropylcellulose films prepared by hot melt extrusion, Drug Development and Industrial Pharmacy 25 (5) (1999) 625–633.
[6] M.M. Crowley, A. Fredersdorf, B. Schroeder, S. Kucera, S. Prodduturi, M.A. Repka, J.W. McGinity, The influence of guaifenesin and ketoprofen on the properties of hot-melt extruded polyethylene oxide films, European Journal of Pharmaceutical Sciences 22 (5) (2004) 409–418.
[7] I. Ozguney, D. Shuwisitkul, R. Bodmeier, Development and characterization of extended release Kollidon (R) SR mini-matrices prepared by hot-melt extrusion, European Journal of Pharmaceutics and Biopharmaceutics 73 (1) (2009) 140–145.
[8] T. Quinten, T. De Beer, C. Vervaet, J.P. Remon, Evaluation of injection moulding as a pharmaceutical technology to produce matrix tablets, European Journal of Pharmaceutics and Biopharmaceutics 71 (1) (2009) 145–154.
[9] G. Verreck, A. Decorte, H.B. Li, D. Tomasko, A. Arien, J. Peeters, P. Rombaut, G. Van den Mooter, M.E. Brewster, The effect of pressurized carbon dioxide as a plasticizer and foaming agent on the hot melt extrusion process and extrudate properties of pharmaceutical polymers, Journal of Supercritical Fluids 38 (3) (2006) 383–391.
[10] Y.C. Zhu, K.A. Mehta, J.W. McGinity, Influence of plasticizer level on the drug release from sustained release film coated and hot-melt extruded dosage forms, Pharmaceutical Development and Technology 11 (3) (2006) 285–294.
[11] C.R. Young, J.J. Koleng, J.W. McGinity, Production of spherical pellets by a hot-melt extrusion and spheronization process, International Journal of Pharmaceutics 242 (1–2) (2002) 87–92.
[12] Q.J. Zhang, W.X. Lin, G. Yang, Q. Chen, Studies on the phase structure of ethylene-vinyl acetate copolymers by solid-state H-1 and C-13 NMR, Journal of Polymer Science Part B – Polymer Physics 40 (19) (2002) 2199–2207.
[13] L.Y. Wang, P.F. Fang, C.H. Ye, J.W. Feng, Solid-state NMR characterizations on phase structures and molecular dynamics of poly(ethylene-co-vinyl acetate), Journal of Polymer Science Part B – Polymer Physics 44 (19) (2006) 2864–2879.
[14] A.M. Henderson, Ethylene-vinyl acetate (EVA) copolymers: a general review, IEEE Electrical Insulation Magazine 9 (1993) 30–38.
[15] P. Tallury, N. Alimohammadi, S. Kalachandra, Poly(ethylene-co-vinyl acetate) copolymer matrix for delivery of chlorhexidine and acyclovir drugs for use in the oral environment: effect of drug combination, copolymer composition and coating on the drug release rate, Dental Materials 23 (4) (2007) 404–409.
[16] S. Kalachandra, D.M. Lin, S. Offenbacher, Controlled drug release for oral condition by a novel device based on ethylene vinyl acetate (EVA) copolymer, Journal of Materials Science – Materials in Medicine 13 (1) (2002) 53–58.
[17] Q.H. Guo, S.R. Guo, Z.M. Wang, Estimation of 5-fluorouracil-loaded ethylene-vinyl acetate stent coating based on percolation thresholds, International Journal of Pharmaceutics 333 (1–2) (2007) 95–102.
[18] P.V. Shastri, Toxicology of polymers for implant contraceptives for women, Contraception 65 (1) (2002) 9–13.
[19] J.A.H. van Laarhoven, M.A.B. Kruft, H. Vromans, In vitro release properties of etonogestrel and ethinyl estradiol from a contraceptive vaginal ring, International Journal of Pharmaceutics 232 (1–2) (2002) 163–173.
[20] B.C. Masschaele, V. Cnudde, M. Dierick, P. Jacobs, L. Van Hoorebeke, J. Vlassenbroeck, UGCT: new X-ray radiography and tomography facility, Nuclear Instruments and Methods in Physics Research A 580 (2007) 266–269.
[21] M. Boone, Y. De Witte, M. Dierick, J. Van den Bulcke, J. Vlassenbroeck, L. Van Hoorebeke, Practical use of the modified Bronnikov algorithm in micro-CT, Nuclear Instruments and Methods in Physics Research B 267 (2009) 1182–1186.
[22] A. Groso, R. Abela, M. Stampanoni, Implementation of a fast method for high resolution phase contrast tomography, Optics Express 14 (18) (2006) 8103–8110.
[23] Y. De Witte, M. Boone, J. Vlassenbroeck, M. Dierick, L. Van Hoorebeke, Bronnikov-aided correction for X-ray computed tomography, Journal of the Optical Society of America A 26 (2009) 890–894.
[24] S. Possemiers, S. Bolca, C. Grootaert, A. Heyerick, K. Decroos, W. Dhooge, D. De Keukeleire, S. Rabot, W. Verstraete, T. Van de Wiele, The prenylflavonoid isoxanthohumol from hops (*Humulus lupulus* L.) is activated into the potent phytoestrogen 8-prenylnaringenin in vitro and in the human intestine, Journal of Nutrition 136 (7) (2006) 1862–1867.
[25] S. Possemiers, K. Verthe, S. Uyttendaele, W. Verstraete, PCR–DGGE-based quantification of stability of the microbial community in a simulator of the human intestinal microbial ecosystem, Fems Microbiology Ecology 49 (3) (2004) 495–507.
[26] L. Li, G. Curran, Determination of Rigid and Mobile Amorphous Content of Semicrystalline Polymers using DSC. Thermal Analysis Application Note, Perkin Elmer Inc., 2006.
[27] E.S. Miller, N.A. Peppas, D.N. Winslow, Morphological-changes of ethylene vinyl acetate-based controlled delivery systems during release of water-soluble solutes, Journal of Membrane Science 14 (1) (1983) 79–92.
[28] R.A. Siegel, J. Kost, R. Langer, Mechanistic studies of macromolecular drug release from macroporous polymers. 1. Experiments and preliminary theory concerning completeness of drug release, Journal of Controlled Release 8 (3) (1989) 223–236.
[29] R.A. Siegel, R. Langer, Mechanistic studies of macromolecular drug release from macroporous polymers. 2. Models for the slow kinetics of drug release, Journal of Controlled Release 14 (2) (1990) 153–167.
[30] M. Donbrow, M. Friedman, Enhancement of permeability of ethyl cellulose films for drug penetration, Journal of Pharmacy and Pharmacology 27 (1975) 633–641.